

Multinucleon transfer reactions for $^{28}\text{Si}+^{90,94}\text{Zr}$ systems in sub and near barrier region

Sunil Kalkal,^{1,*} S. Mandal,¹ N. Madhavan,² A. Jhingan,² E. Prasad,³ Rohit Sandal,⁴ S. Nath,² J. Gehlot,² Ritika Garg,¹ Gayatri Mohanto,² Mansi Saxena,¹ Savi Goyal,¹ S. Verma,¹ B. R. Behera,⁴ T. Varughese,² Suresh Kumar,¹ U. D. Pramanik,⁵ K. S. Golda,² S. Muralithar,² A. K. Sinha,⁶ R. Singh¹

¹*Department of Physics & Astrophysics, University of Delhi-110007.*

²*Inter University Accelerator Centre, New Delhi.*

³*Department of Physics, Calicut University, Kerala.*

⁴*Department of Physics, Panjab University, Chandigarh.*

⁵*Saha Institute of Nuclear Physics, Kolkata.*

⁶*UGC-DAE Consortium for Scientific Research, Kolkata.*

* email: kalkal84@gmail.com

Measurements were performed for the multi-nucleon transfer reactions for $^{28}\text{Si}+^{90,94}\text{Zr}$ systems at sub and near barrier energies. The studies revolve around the quantitative effect of transfer channel couplings on the fusion cross sections around the Coulomb barrier. The fact that ^{90}Zr has closed neutron shell and ^{94}Zr has four neutrons outside the closed shell, allows us to investigate the effects of shell closure and pairing correlations on multi-nucleon transfer mechanism. The experiment was performed with pulsed ^{28}Si beam using Heavy Ion Reaction Analyzer (HIRA) at IUAC, New Delhi. Kinematic coincidence was set up to reduce the background. At the target chamber, 14 elements BGO array was mounted for gamma detection in coincidence with recoils to obtain ground state and excited state transfer strengths. We could clearly resolve m/q ambiguity by time of flight technique. From Q-value considerations, it turned out that pick-up channels were neutron transfer whereas stripping channels were proton transfer. In case of $^{28}\text{Si}+^{94}\text{Zr}$, slope parameter is almost same for two, three and four nucleon pick-up channels. In case of $^{28}\text{Si}+^{90}\text{Zr}$, the slope parameter for two neutron pick-up is less than one neutron pick-up. The experimental and theoretical excitation energy spectra (using GRAZING) match reasonably well for both the systems.

PACS number(s): 25.70.Hi

I. Introduction

Heavy ion collisions around the Coulomb barrier offer a very rich variety of phenomena and their coupling effects on each other [1, 2]. It is in this energy regime where transfer reactions constitute a significant part of reaction cross section. In spite of debate in the last few decades, the role of multi nucleon transfer channels in sub-barrier fusion cross section is not very clear [3-5]. One of the reasons for that is properly including all the open channels in coupled channel formalism [6, 7] in heavy ion collisions. The study of transfer reactions in itself serves a wide range of objectives like estimation of relative and absolute spectroscopic factors of nuclear levels [8], understanding correlations between nucleons [9], the transition from the quasi elastic to deep inelastic regime [1], dynamics of neck formation. These reactions can also be used to populate high spin states of nuclei as a large amount of angular momentum is transferred both from the relative orbital angular momentum as well as internal motion of nucleons along with mass and charge in multi-nucleon transfer reactions [10-12]. These reactions are very useful tool to study exotic nuclei far off from the stability line [13, 14]. Information about these nuclei may be very helpful in understanding the change in collective properties with increase or decrease of neutron-proton ratio. Multi nucleon transfer can take place either simultaneously or sequentially showing the interplay of reactions and nuclear structure. But unfortunately the mechanism and many features of multi nucleon transfer reactions are still not very well understood [8, 9, 15, 16]. Multi nucleon transfer is a multistep transfer in which the colliding nuclei can be inelastic excited before or after the transfer in addition to the simultaneous transfer as a cluster. The number of such possibilities increases drastically with increasing number of nucleon getting transferred and the establishment of reaction mechanism in such a condition becomes very tedious job. So far, it has not been possible to estimate the relative importance of sequential and simultaneous transfer in multi-nucleon transfer reactions.

In the sub-barrier region, very scarce data exist for the measurement of multi-nucleon transfer reactions due to various technical difficulties faced in these kinds of reactions [17-23]. The transfer cross sections are very low in the sub-barrier region and there will be huge elastic cross section in this energy region. The reaction products in these kinds of reactions are backward peaked (180°) in centre of mass system and forward moving recoils are peaked at zero

degree. Moreover, the energy of forward moving recoils as well as back scattered particles is less than 1 MeV/nucleon, so the detection of the particles in these kinds of reactions is very cumbersome. Hence, a recoil mass separator is very efficient device for carrying out these kind of measurements. The measurement of these reactions in the sub-barrier region helps in understanding the interplay of various channels like elastic, inelastic, transfer and fusion with each other [24].

The role of one and two nucleon transfer in the sub-barrier fusion enhancement has been established more or less but the role of multinucleon transfer is still not studied very well. Very few data exist on the role of multinucleon transfer on the sub-barrier fusion cross section enhancement [25-28]. As the coupling effects are maximum in sub-barrier region; so these measurements were carried out in this region only. Here we report the results of measurements of multi-nucleon transfer for $^{28}\text{Si} + ^{90,94}\text{Zr}$ systems at near barrier energies. The studies revolve around the interplay of transfer reactions channels (mainly positive Q value multi neutron pick-up) and the fusion cross sections around the Coulomb barrier. For these systems, we have already carried out fusion cross section measurements [29]. As ^{90}Zr has closed neutron shell, the effect of shell closure on neutron transfer can be studied. On the other hand, ^{94}Zr has four nucleons outside the closed shell, one can investigate the effects of pairing correlation on multi-nucleon transfer mechanism. The enhancement observed for even number of nucleon transferred has been a very controversial topic. It is observed in some cases [30-32] and was not observed in some systems [33-35] for neutron transfer. In the cases where enhancement was not observed it was found that for each successive neutron transfer the cross section was falling by a factor of 3-5 and no enhancement in the cross sections for 2n, 4n, 6n with respect to 1n, 3n, 5n is observed. The enhancement for even number of pair transfer has also been observed for proton transfer in some cases [36-38].

II. Experimental details

The experiment was performed with pulsed ^{28}Si beam having a repetition rate of $1\mu\text{s}$ using Heavy Ion Reaction Analyzer (HIRA) [39] at IUAC, New Delhi. The targets used were isotopically enriched $^{90,94}\text{Zr}$ (97.65% and 96.07% respectively) $280\mu\text{g}/\text{cm}^2$ foils prepared on $45\mu\text{g}/\text{cm}^2$ carbon backings in the target lab of IUAC [40]. In the target chamber of HIRA, two

silicon surface barrier detectors were mounted at $\pm 25^\circ$ to monitor the beam. To improve the beam rejection, HIRA was rotated to 6° . A silicon surface barrier detector of $20 \times 20 \text{ mm}^2$ active

area was mounted at back angle to set-up kinematic coincidence between forward moving target-like recoiling particles and back scattered projectile-like nuclei. The angle of this back detector was optimized by maximizing the coincidence counts. At the target chamber of HIRA, 14 elements BGO array was also mounted for gamma detection in coincidence with recoils. A carbon charge reset foil of $30 \mu\text{g}/\text{cm}^2$ thickness was used for charge equilibration of recoiling particles coming out of the target. At the focal plane of HIRA, a Multi Wire Proportional

Counter (MWPC) of $150 \times 50 \text{ mm}^2$ active area followed by ionization chamber was used for the

detection of recoiling particles. The timing information (TOF) was obtained with arrival of particles at focal plane MWPC as start and RF of the beam as stop to separate multiply scattered beam-like and recoiling target-like particles at the focal plane. One more TAC (MWPC-SSB-TAC) was defined taking MWPC anode signal as start and delayed back-angle SSBD signal as stop. This was very much helpful in removing the beam like background at all. Forward moving recoils were dispersed according to their m/q values at the focal plane of HIRA. The measurements were performed at 83.3, 86.4, 89.5, 92.5 and 95.5 MeV (in laboratory frame E_{lab}). The nominal Coulomb barriers for $^{28}\text{Si}+^{90,94}\text{Zr}$ are 95.76 and 94.15 MeV (E_{lab}) respectively. The

solid angle of acceptance for HIRA was kept 5 mSr ($6^\circ \pm 2.28^\circ$) for carrying out all these

measurements. A gated two dimensional spectra between the time of flight (TOF) vs. MWPC position for $^{28}\text{Si}+^{94}\text{Zr}$ at 94 MeV is shown in Fig. 1. This spectrum was gated by ER-RF-TAC

and MWPC-SSBD-TAC both. Fig. 2 shows the projected mass spectrum of recoiling target like particles for $^{28}\text{Si}+^{94}\text{Zr}$ at 97 MeV. The transfer of up to 4-nucleon pick-up and one nucleon stripping can be noted in Figs 1 and 2. We could clearly resolve m/q ambiguity by time of flight. As the energy of the forward recoiling target-like particles was much less than 1 MeV/nucleon, so Z-identification was not possible. From the Q-value considerations it was found that pick-up channels were neutron transfer whereas stripping channels were proton transfer. A list of the ground state Q-values for various transfer channels is given in Table 1. An extreme low energy run was taken at 70 MeV (much below the Coulomb barrier so that transfer does not take place significantly) to determine the isotopic contents of the targets experimentally. The values so obtained were found to be consistent with the values provided by supplier. For optimising the HIRA transmission efficiency, the energy distribution, charge state distribution was scanned. To get position dependent efficiency factor, HIRA was scanned for different masses/positions of the focal plane and this mass correction factor was incorporated while extracting the transfer probability.

III. Results and Discussion

At the focal plane of the HIRA, transfer products along with the elastic recoils are focused according to their m/q values. As the solid angle factor is same for all the channels, so the yields of these channels can be directly used for extracting the transfer probabilities. The transfer probability was taken as the ratio of the yield of that particular transfer channel to the total yield of elastic, inelastic and transfer channels (quasielastic yield) i.e.

$$P_{tr} = \frac{Y_{tr}}{Y_{qe}}$$

The mass correction factor was taken into account while extracting the transfer probability. The transfer probability of one nucleon pick-up for ^{94}Zr was found to be almost an order of magnitude higher than ^{90}Zr at each energy, which is a convincing evidence of the role of transfer channels in the enhancement of fusion cross sections. The main transfer channels observed with ^{94}Zr target were upto four nucleon pick-up and one nucleon stripping whereas in the case of ^{90}Zr only upto two neutron pick-up channels could be observed with non-negligible probabilities. In the present measurements, data was taken mostly in the sub-barrier region (sommerfield parameter being $\gg 1$), so semiclassical formalism [8, 9] of scattering can be applied. It can be

assumed that the incident particle follows the Coulomb trajectory and the transfer probability is maximum at the distance of closest approach. In this region, the effect of nuclear interaction can be neglected. Here the distance of closet approach is defined as (assuming pure Coulomb trajectory)

$$D = \frac{Z_p Z_T e^2}{2E_{c.m.}} \left(1 + \cos ec \frac{\theta_{c.m.}}{2} \right) = d_0 \left(A_p^{1/3} + A_T^{1/3} \right)$$

Here, $E_{c.m.}$ is the energy of the incident particles in the centre of mass system and $\theta_{c.m.}$ is the angle of the projectile like particles in the centre of mass system and d_0 is the distance parameter. The nuclear effects are neglected here as they were found to be insignificant for $d_0 > 1.5 \text{ fm}$. In Figs. 3 and 4 the transfer probabilities extracted so vs. the distance parameter are plotted for $^{28}\text{Si} + ^{90,94}\text{Zr}$ systems respectively. Since the transfer reactions take place by tunneling through the barrier between the colliding nuclei in the sub-barrier region, so exponential dependence of the transfer probabilities on the distance of closet approach can be assumed. The probability curves in the fig. were fitted using the expression

$$P_{tr}(D) = P_{tr}(R_B) \exp[-2\alpha(D - R_B)]$$

Where $P_{tr}(R_B)$ is the transfer probability at the barrier radius and $R_B (1.4(A_p^{1/3} + A_T^{1/3}))$ is the barrier radius. Theoretically, the slope parameter was taken average of the slope parameters of the donor and acceptor nuclei. The slope parameter was defined as

$$\alpha = \frac{1}{2}(\alpha_i + \alpha_f); \alpha_k = \sqrt{\frac{2\mu_k(E_B)_k}{\hbar^2}}$$

where μ is the reduced mass of the donor or acceptor nucleus and E_B is the effective binding

energy of the transferred nucleons. The effective binding energy for neutron transfer is same as the binding energy as these particles don't feel any Coulomb force but for proton transfer the effective binding energy was taken as [41]

$$E_B = E_B^0 - \Delta V + V_C$$

ΔV is the change in the binding energy due to the Coulomb field of the approaching collision partner and V_c is the Coulomb barrier that the transferred particle has to overcome.

The values of the slope parameter obtained experimentally along with the theoretically calculated values are listed in Table 2. Also, the transfer probabilities at the barrier radius obtained by fitting transfer probability vs. distance parameter are listed. It is found that for both the systems, the transfer probability at the barrier radius for 2n is almost half for that of 1n. The transfer probability for 3n is but a factor of 5 smaller than that of 2n. Some kind of odd-even staggering was observed in these systems which could be due to pairing correlations. This suggests the contributions from the simultaneous transfer in addition to sequential transfer for multi-nucleon transfer reactions. Moreover, the transfer probability for one neutron pick-up channel for $^{28}\text{Si}+^{94}\text{Zr}$ system was a factor of two higher as compared to one proton stripping which could be due to sub-shell closure for protons. For the $^{28}\text{Si}+^{94}\text{Zr}$, the experimental slope is constant after 2n pick up. Same was observed in the case of $^{58}\text{Ni}+^{124}\text{Sn}$ [22] where slope was constant after three neutron pick up to upto six neutron pick-up. In the same table, the values of the transfer form factors extracted experimentally at the barrier radius are also given. For the extraction of the transfer form factor, the first order perturbation approximation was used. In this approximation, for a transfer channel β (corresponding to particular states of the final nuclei) with Q_β transfer Q-value; the transfer probability is related to the transfer form factor as [42]

$$P_{tr}(r_0, Q_\beta) = \frac{\pi}{\sigma^2} |F_\beta(r_0, Q_\beta)|^2 \exp\left[\frac{-(Q_\beta - Q_{opt})^2}{2\sigma^2}\right]$$

Where Q_{opt} is the optimum Q-value for transfer to take place, σ is the width of the Q-value

distribution (standard deviation). Here σ and Q_{opt} are given by

$$\sigma = \sqrt{\frac{\alpha \hbar^2 \ddot{r}}{2}}; \quad \ddot{r} = \frac{2E_{c.m.} - E_B}{m_{aA} R_B}$$

$$Q_{opt} = \left(\frac{Z_p^f Z_T^f}{Z_p^i Z_T^i} - 1 \right) E_{c.m.}$$

Here $E_{c.m.}$ is the energy in the centre of mass system, α is the slope parameter obtained

experimentally, \ddot{r} is the acceleration at the turning point and m_{aA} is the reduced mass and E_B is the barrier height and R_B is the barrier radius. In the expression for Q_{opt} , f is used for the final channel and i is used for the incident channel and Z_p and Z_T is atomic no. of projectile and target respectively. The Q_{opt} value is zero for neutron transfer channels. As the resolution of the detector was not good enough to resolve states of the nuclei so if the transfer probability is integrated over the Q values then the expression for transfer probability becomes

$$P_{tr}(r_0) = \frac{\pi}{\sigma^2} \frac{d|F_\beta(r_0)|^2}{dQ} \int_{-\infty}^{Q_{gs}} \exp\left[-\frac{(Q_\beta - Q_{opt})^2}{2\sigma^2}\right] dQ.$$

So, a Q-value independent form factor is obtained. By fitting curve of P_{tr} vs. D one obtains the slope parameter and the value of transfer probability at the barrier radius. So using that value of the transfer probability, from the above expression ne can obtain the value of F_0 which can be

defined as $F_0 = \sqrt{\frac{d|F(r_0)|^2}{dQ}}$. The values of the form factor so obtained are listed in Table 2.

Figs. 5 and 6 show the excitation energy spectrum for both the systems at lowest and highest energies at which data was taken (83.3 MeV and 95.5 MeV respectively). The back angle SSBD was calibrated for scattered Si-like particles with respect to the elastically scattered silicon. Using this calibration the energy of the back scattered particles was obtained. The excitation energy of these nuclei was calculated by taking difference between energy of scattered particles for ground state transfer and energy spectrum obtained experimentally. In these Figs. the step line shows the experimental excitation energy spectrum obtained whereas the continuous line shows the excitation energy spectrum obtained by using code GRAZING [43]. The dotted line is

for 83.3 MeV whereas the solid line is for 95.5 MeV. GRAZING is based on semiclassical theory [44] and it gives the capture, quasi elastic and transfer cross sections along with the angular distribution, Q value distribution of transfer channels after collision. This code includes independent single particle transfer for multi nucleon transfer reactions and also includes the inelastic excitation to the low lying states. However, it does not include cluster transfer in case of multi-nucleon transfer channels i.e. simultaneous transfer of nucleons is not considered only sequential transfer is assumed. It also takes into account the effects of neutron evaporation from the primary fragments.

From the Fig. 6, it is clear that for $^{28}\text{Si}+^{94}\text{Zr}$, the experimental and theoretical values match very well for one and two-nucleon transfer reactions (1n and 2n pick-up and 1p stripping) at 95.5 Me. However at 83.3 MeV, the theoretical two neutron pick-up excitation energy distribution deviates slightly from experimentally obtained spectrum. At this energy, GRAZING predicts the high excitation energy spectrum as compared to experimental data. For three and four neutron pick-up channels, there is some discrepancy between theoretical and experimental spectrum for both energies. For three neutron pick-up, the theoretical values are predicting the excitation energy higher than the experimental values and for four neutron transfer the deviation is still more. GRAZING doesn't predict four neutron pick-up channel at 83.3 MeV but was observed experimentally. It seems as if the transfer is taking place from the ground state to the ground state and hence peaking at zero excitation energy. However, at 95.5 MeV, for one and two neutron pick-up, the excitation energy spectrum is peaking at slightly higher excitation energy which may be due to the excited state transfer. But at 83.3 MeV, one neutron transfer peaks at zero excitation energy. Here, it is to be mentioned that GRAZING doesn't include simultaneous transfer which may be an important mechanism of multi-nucleon transfer channels and that may be the reason for the deviation observed for multi-nucleon transfer in this case at sub-barrier energies. The excitation energy spectrum is broader at 93.5 MeV as compared to 83.3 MeV which gives clear evidence that cold transfer (from ground state to ground state) is dominant mechanism of transfer at 83.3 MeV.

For $^{28}\text{Si}+^{90}\text{Zr}$, the theory predicts pretty well for one neutron transfer but starts deviating for two neutron transfer and predicts pretty high excitation energy for three neutron transfer channel at 95.5 MeV. However at 85.3 MeV, even for one neutron pick-up channel theory and experimental spectrum doesn't match at all which could be due to the negative ground state Q-

value. At this energy, the transfer mainly occurs at the optimum Q-value for all the transfer channels. Three neutron pick-up was not observed at 85.3 MeV. Similar to $^{28}\text{Si}+^{94}\text{Zr}$, the excitation energy spectrum is narrower at 85.3 MeV as compared to 95.5 MeV. From experimental spectrum, it looks as if three nucleon transfer is taking place at the optimum Q-value owing to the high negative Q-value for ground state transfer. No specific broadening of the excitation energy spectrum for the multi nucleon transfer is observed giving clear evidence that in the sub barrier region the transfer occurs from ground state to ground state. So, the excitation energy of spectra does not increase to high excitation energies with increasing number of nucleons getting transferred. The reason for that may be that all these measurements were done just below the barrier.

In Fig. 7, the transfer probability values for various transfer channels obtained experimentally are compared with the theoretically obtained values using GRAZING neglecting and considering the evaporation of nucleons from the fragments. No normalization was needed to match the one nucleon transfer probability. However, the multi-nucleon transfer probabilities are much more enhanced as compared to the theoretically predicted values.

IV. Summary and Conclusion

The results of multi-nucleon transfer reactions studied for $^{28}\text{Si}+^{90,94}\text{Zr}$ systems are reported here. For $^{28}\text{Si}+^{94}\text{Zr}$ system, upto four nucleon pick-up and one nucleon stripping was observed. From the Q-value considerations, it was found that the nucleon pick-up channels were neutron transfer channels except four nucleon transfer channel in which some contamination from the alpha pick-up channel may be there as the Q-value spectrum for four neutron pick-up was narrower as compared to two and three nucleon transfer channels. From the excitation spectrum, it was also observed that the excitation energy spectra become broader as the beam energy is increased which may be due to excited state transfer taking place at higher energy. Also, it was observed that when the transfer channel Q-value is positive as in the case of $^{28}\text{Si}+^{94}\text{Zr}$, then transfer takes place mainly at the ground state Q-value but if it is negative as in the case of $^{28}\text{Si}+^{90}\text{Zr}$, then the transfer takes place mainly at the optimum Q-value. From the results reported here, it can be concluded that the simultaneous transfer is also an important mechanism of multi-nucleon transfer reactions at the sub-barrier energies which may be due to pairing correlations being stronger in the ground state transfer. Another evidence of pairing correlations observed in

these systems is the odd even staggering observed for multi-nucleon transfer probabilities at the barrier radius.

References

- [1] K. E. Rehm , Annu. Rev. Nucl. Part. Sci. **41**, 429 (1991).
- [2] W. Reisdorf, J. Phys. G **20**, 1297 (1994).
- [3] M. Dasgupta, D. J. Hinde, N. Rowley, A. M. Stefanini, Annu. Rev. Nucl. Part. Sci. **48**, 401 (1998).
- [4] H. Timrners, L. Corradi, A. M. Stefanini, D. Ackermann, J. H. He, S. Beghini, G. Montagnoli, F. Scarlassara, G. F. Segato, N. Rowley, Phys. Lett. **B399**, 35 (1997).
- [5] A. A. Sonzogni, J. D. Bierman, M. P. Kelly, J. P. Lestone, J. F. Liang, R. Vandenbosch, Phys. Rev. C **57**, 722 (1998).
- [6] T. Tamura, Annu. Rev. Nucl. Part. Sci. **19**, 99 (1969).
- [7] Taro Tamura, Rev. Mod. Phys. **37**, 679 (1965).
- [8] C. Y. Wu, W. Von Oertzen, D. Cline, M. W. Guidry, Annu. Rev. Nucl. Part. Sci. **40**, 285 (1990).
- [9] W. Von Oertzen, A. Vitturi, Rep. Prog. Phys. **64**, 1247 (2001).
- [10] A. N. Wilson, C. W. Beausang, N. Amzal, D. E. Appelbe, S. Asztalos, P. A. Butler, R. M. Clark, P. Fallon, A.O. Macchiavelli, Eur. Phys. J. A **9**, 183 (2000).
- [11] C. Wheldon, J. J. Valiente-Dob'ón, P. H. Regan, C. J. Pearson, C. Y. Wu, J. F. Smith, A. O. Macchiavelli, D. Cline, R. S. Chakrawarthy, R. Chapman, M.. Cromaz, P. Fallon, S. J. Freeman, A. G. orgen, W. Gelletly, A. Hayes, H. Hua, S. D. Langdown, I. Y. Lee, X. Liang, Zs. Podoly'ak, G. Sletten, R. Teng, D. Ward, D. D. Warner, A. D. Yamamoto, Eur. Phys. J. A **20**, 365 (2004).
- [12] M. W. Guidry, S. Juutinen, X. T. Liu, C. R. Bingham, A. J. Larabee, L. L. Riedinger, C. Baktash, I. Y. Lee, M. L. Halbert, D. Cline, B. Kotlinski, W. J. Kernan, T. M. Semkow, D. G. Sarantites, K. Honkanen, M. Rajgopalan, Phys. Lett. **B163**, 79 (1985).
- [13] H. Lenske, G. Schrieder, Eur. Phys. J. A **2**, 41 (1998).
- [14] Yu. E. Penionzhkevich, G. G. Adamian, N. V. Antonenko, Phys. Lett. **B621**, 119 (2005).
- [15] W. R. Philips, Rep. Prog. Phys. **40**, 345 (1977).
- [16] L. Corradi, G. Pollarolo, S. Szilner, J. Phys. G **36**, 113101 (2009).
- [17] C. N. Pass, P. M. Evans, A. E. Smith, L. Stuttge, R. R. Betts, J. S. Lilley, D. W. Banes, K. A. Connel, J. Simpson, J. R. Smith, A. N. James, Nucl. Phys. **A499**, 173 (1989).
- [18] K. E. Rehm, C. L. Jiang, J. Oehring, B. Olagola, W. Kutschera, M. D. Pdaein, A. H. Wuosmaa , Nucl. Phys. **A583**, 421 (1995).

- [19] R. R. Betts, P. M. Evans, C. N. Pass, N. Poffe, A. E. Smith, L. Stuttge, J. S. Liley, D. W. Banes, K. A. Connell, J. Simpson, J. R. H. Smith, A. N. James, B. R. Fulton, Phys. Rev. Lett. **59**, 978 (1987).
- [20] L. Corradi, A. M. Stefanini, D. Ackerman, S. Beghini, G. Montagnoli, C. Petrache, F. Scarlassara, C. H. Dasso, G. Pollarolo, A. Winther, Phys. Rev. C **49**, R2875 (1994).
- [21] M. Devlin, D. Cline, R. Ibbotson, M. W. Simon, C. Y. Wu, Phys. Rev. C **53**, 2900 (1996).
- [22] C. L. Jiang, K. E. Rehm, H. Esbensen, D. J. Blumenthal, B. Crowell, J. Gehring, B. Glagola, J. P. Schiffer, and A. H. Wuosmaa, Phys. Rev. C **57**, 2393 (1998).
- [23] D. O. Kataria, A. K. Sinha, J. J. Das, N. Madhavan, P. Sugathan, Lagy. T. Baby, I. Mazumdar, R. Singh, C. V. K. Baba and Y. K. Agarwal, A. M. Vinodkumar and K. M. Varier, Phys. Rev. C **56**, 1902 (1997).
- [24] L. Corradi, S. J. Skorka, T. Winkelmann, K. Balog, P. Jiinker, H. Leitz, U. Lenz, K. E. G. Lobner, K. Rudolph, M. Steinmayer, H. G. Thies, B. Million, D. R. Napoli, A. M. Stefanini, S. Beghini, G. Montagnoli, F. Scarlassara, C. Signorini, F. Soramel, Z. Phys. A **346**, 217 (1993).
- [25] C. R. Morton, M. Dasgupta, D. J. Hinde, J. R. Leigh, R. C. Lemmon, J. P. Lestone, J. C. Mein, J. O. Newton, H. Timmers, N. Rowley, A. T. Kruppa, Phys. Rev. Lett. **72**, 4074 (1994).
- [26] H. Timmers, L. Corradi, A. M. Stefanini, D. Ackermann, J. H. He, S. Beghini, G. Montagnoli, F. Scarlassara, G. F. Segato, N. Rowley, Phys. Lett. **B399**, 35 (1997).
- [27] G. Montagnoli, S. Beghini, F. Scarlassara, A. M. Stefanini, L. Corradi, C. J. Lin, G. Pollarolo, Aage Winther, Eur. Phys. J. A **15**, 351 (2002).
- [28]
- [29] Sunil Kalkal, S. Mandal, N. Madhavan, E. Prasad, Shashi Verma, A. Jhingan, Rohit Sandal, S. Nath, J. Gehlot, B. R. Behera, Mansi Saxena, Savi Goyal, Davinder Siwal, Ritika Garg, U. D. Pramanik, Suresh Kumar, T. Varughese, K. S. Golda, S. Muralithar, A. K. Sinha, R. Singh (submitted in Phys. Rev. C.)
- [30] I. Peterl, W. von Oertzen, H. G. Bohlen, A. Gadea, B. Gebauer, J. Gerl, M. Kaspar, I. Kozhoukharov, T. KrÄoll, M. Rejmund, C. Schlegel, S. Thummerer, H. J. Wollersheim, Eur. Phys. J. A **4**, 313 (1999).
- [31] W. Donnweber, H. Morinaga, D. E. Alburger, Phys. Lett. **B106**, 47 (1981).
- [32] W. von Oertzen, H. G. Bohlen, B. Gebauer, R. Kunkel, F. Puhlhofer, D. Schiill, Z. Phys. A **326**, 463 (1987).
- [33] G. Montagnoli, S. Beghini, F. Scarlassara, G. F. Segato, L. Corradi, C. J. Lin, A. M. Stefanini, J. Phys. G **23**, 1431 (1997).

- [34] L. Corradi, J. H. He, D. Ackermann, A. M. Stefanini, and A. Pisent, S. Beghini, G. Montagnoli, F. Scarlassara, and G. F. Segato, G. Pollarolo, C. H. Dasso, A. Winther, Phys. Rev. C **54**, 201(1996).
- [35] C. L. Jiang, K. E. Rehm, J. Gehring, B. Glagola, W. Kutschera, M. Rhein, A. H. Wuosmaa, Phys. Lett. **B337**, 59 (1994).
- [36] R. Kunkel, W. von Oertzen, H. G. Bohlen, B. Gebauer, H.A. B6sser, B. Kohlmeyer, J. Speer, F. Puhlhofer, D. Schiill, Z. Phys. A **336**, 71 (1990).
- [37] J. Speer, W. von Oertzen, D. Schiill, M. Wilpert, H.G. Bohlen, B. Gebauer, B. Kohlmeyer, F. Puhlhofer, Phys. Lett. **B259**, 422 (1991).
- [38] Thomas Wilpert, B. Gebauer, M. Wilpert, H. G. Bohlen, W. von Oertzen, Z. Phys. A **358**, 395 (1997).
- [39] A. K. Sinha, N. Madhavan, J. J. Das, P. Sugathan, D. O. Kataria, A. P. Patro, G. K. Mehta, Nucl. Instrum. Methods Phys. Res. A **339**, 543 (1994).
- [40] Sunil Kalkal, S. R. Abhilash, D. Kabiraj, S. Mandal, N. Madhavan, R. Singh, Nucl. Instrum. Methods Phys. Res. A **613**, 190 (2010).
- [41] L. Corradi, S. J. Skorka, U. Lenz, K. E. G. Liibner, P. R. Pascholati, U. Quade, K. Rudolph, W. Schomburg, M. Steinmayer, H. G. Thies, G. Montagnoli, D. R. Napoli, A. M. Stefanini, A. Tivelli, S. Beghini, F. Searlassara, C. Signorini, F. Soramel, Z. Phys. A **334**, 55 (1990).
- [42] S. Saha, Y. K. Agarwal, C. V. K. Baba, Phys. Rev. C **49**, 2578 (1994).
- [43] A. Winther, GRAZING, computer program (may be downloaded from <http://www.to.infn.it/~nanni/grazing>).
- [44] Aage Winther, Nucl. Phys. **A572**, 191 (1994), Nucl. Phys. **A594**, 203 (1995).

Table Captions:

TABLE I. Ground state Q-values for the various transfer channels for $^{28}\text{Si}+^{90,94}\text{Zr}$ systems.

TABLE II. Transfer probabilities for various channels at the barrier radius (R_B), experimentally

extracted slope parameter (α_{expt}), theoretically calculated slope parameter (α_{th}) and the form

factor for $^{28}\text{Si}+^{90,94}\text{Zr}$ systems.

Figure Captions:

FIG. 1. A two-dimensional spectrum of $^{28}\text{Si}+^{94}\text{Zr}$ at 94 MeV.

FIG. 2. A one dimensional projection of $^{28}\text{Si}+^{94}\text{Zr}$ at 97 MeV.

FIG. 3. P_{tr} vs. distance parameter (d_0) for $^{28}\text{Si}+^{90}\text{Zr}$.

FIG. 4. P_{tr} vs. distance parameter (d_0) for $^{28}\text{Si}+^{94}\text{Zr}$.

FIG. 5. Excitation energy distribution of projectile-like particles for $^{28}\text{Si}+^{90}\text{Zr}$ at 97 MeV. The red line is for 85 MeV and the black line is for 97 MeV. The step function is for experimental distribution whereas the smooth line is for GRAZING calculations.

FIG. 6. Excitation energy distribution of projectile-like particles for $^{28}\text{Si}+^{94}\text{Zr}$ at 97 MeV. The red line is for 85 MeV and the black line is for 97 MeV. The step function is for experimental distribution whereas the smooth line is for GRAZING calculations.

FIG. 7. Transfer probability for various transfer channels for $^{28}\text{Si}+^{94}\text{Zr}$ at 97 MeV. The theoretical calculations are performed using code GRAZING. The red line shows GRAZING calculations after taking particle evaporation into account whereas the black line shows same without considering particle evaporation.

TABLE I.

System	Channel	Q _{g.s.} (MeV)	Channel	Q _{g.s.} (MeV)	Channel	Q _{g.s.} (MeV)
²⁸ Si+ ⁹⁴ Zr	+1n	0.252	-1p	-4.781	+2p1n	-6.070
	+2n	4.127	-1n	-10.718	+1p3n	2.033
	+3n	2.080	+1p1n	-3.746	+2p2n	3.198
	+4n	4.088	+1p2n	2.026	+3p1n	-16.068
²⁸ Si+ ⁹⁰ Zr	+1n	-3.496	+3n	-7.963	+1p2n	-2.800
	+2n	-2.204	+1p1n	-5.760	+2p1n	-6.335

TABLE II.

System	Channel	P _{tr} (R _B)	α _{th}	α _{expt}	F ₀
		0.2037±0.0061		0.3908±0.0141	
²⁸ Si+ ⁹⁴ Zr	+1n		0.6247		0.2732

+2n	0.1053 ± 0.0026	1.2449	0.6317 ± 0.0135	0.1679
+3n	0.0188 ± 0.0012	1.8174	0.6014 ± 0.0346	0.0752
+4n	0.0188 ± 0.0011	2.3958	0.6163 ± 0.0303	0.0705
-1p	0.0984 ± 0.0073	0.6853	0.6801 ± 0.0409	0.3078

		0.0728 ± 0.0084	0.4922 ± 0.0401	
$^{28}\text{Si} + ^{90}\text{Zr}$	+1n		0.6891	0.7798

		0.0367 ± 0.0037	0.3453 ± 0.0331	
	+2n		1.3581	0.3086

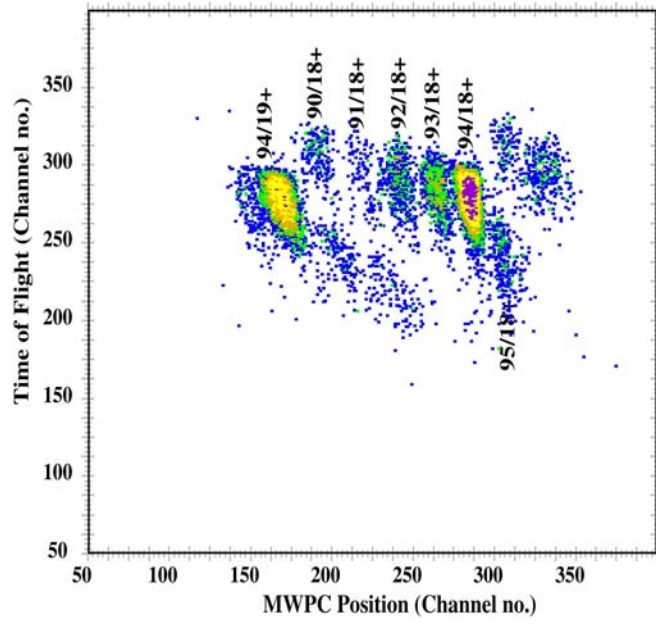


FIG. 1. (Color Online)

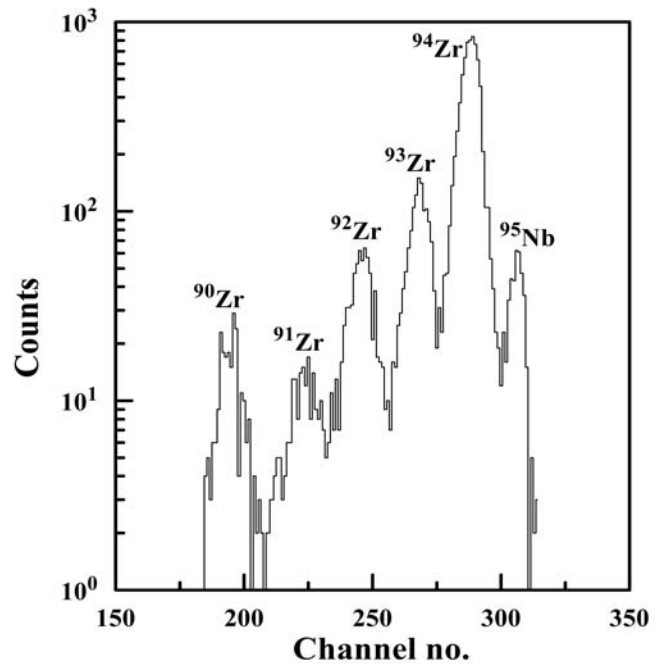


FIG. 2.

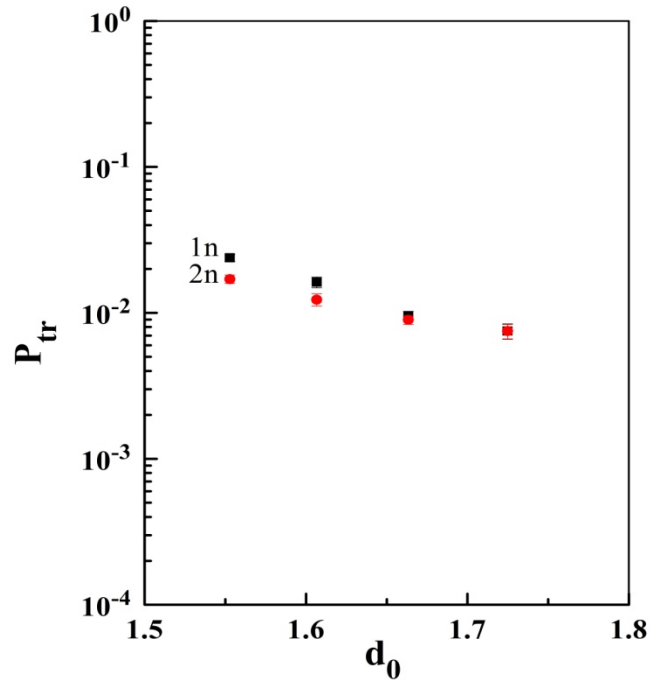


FIG. 3.

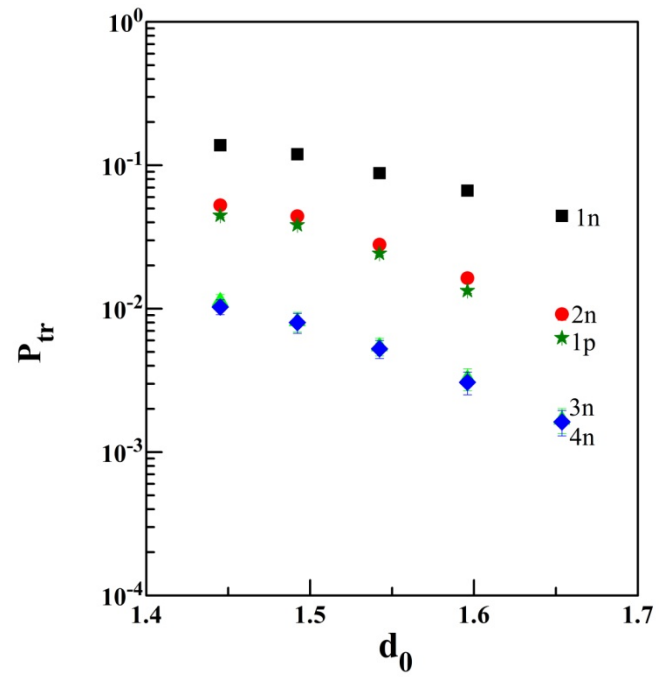


FIG. 4.

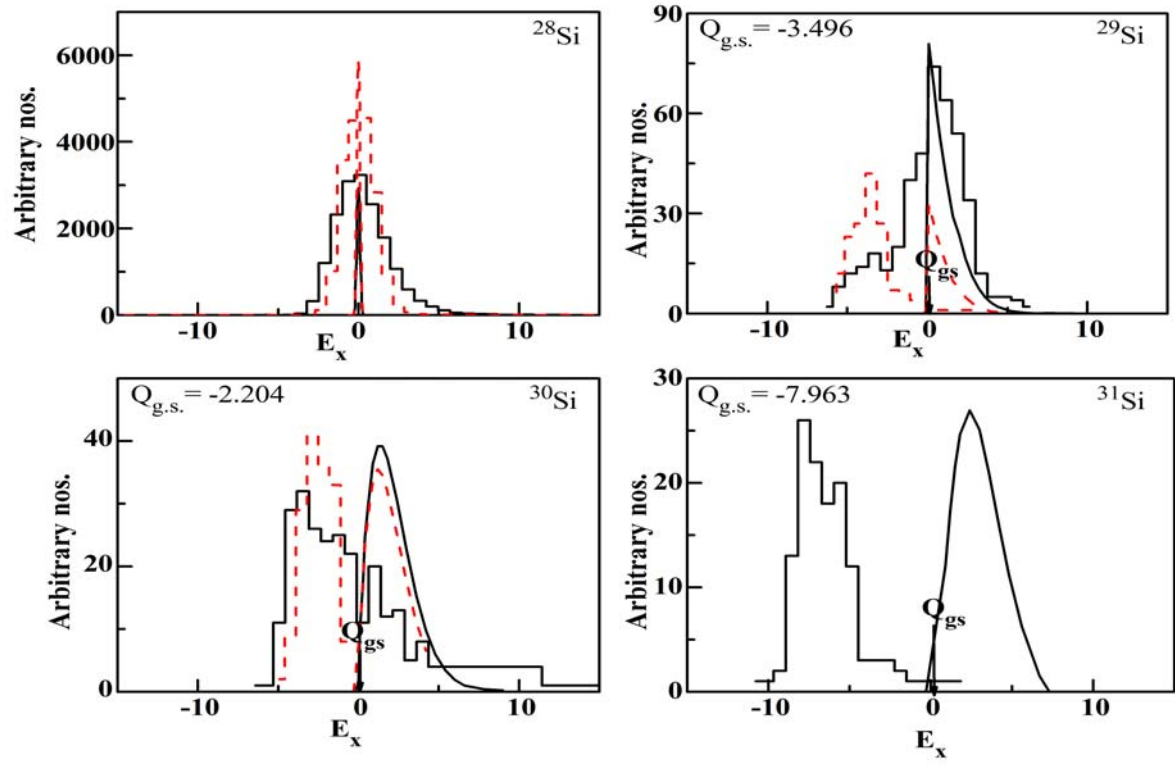


FIG. 5.

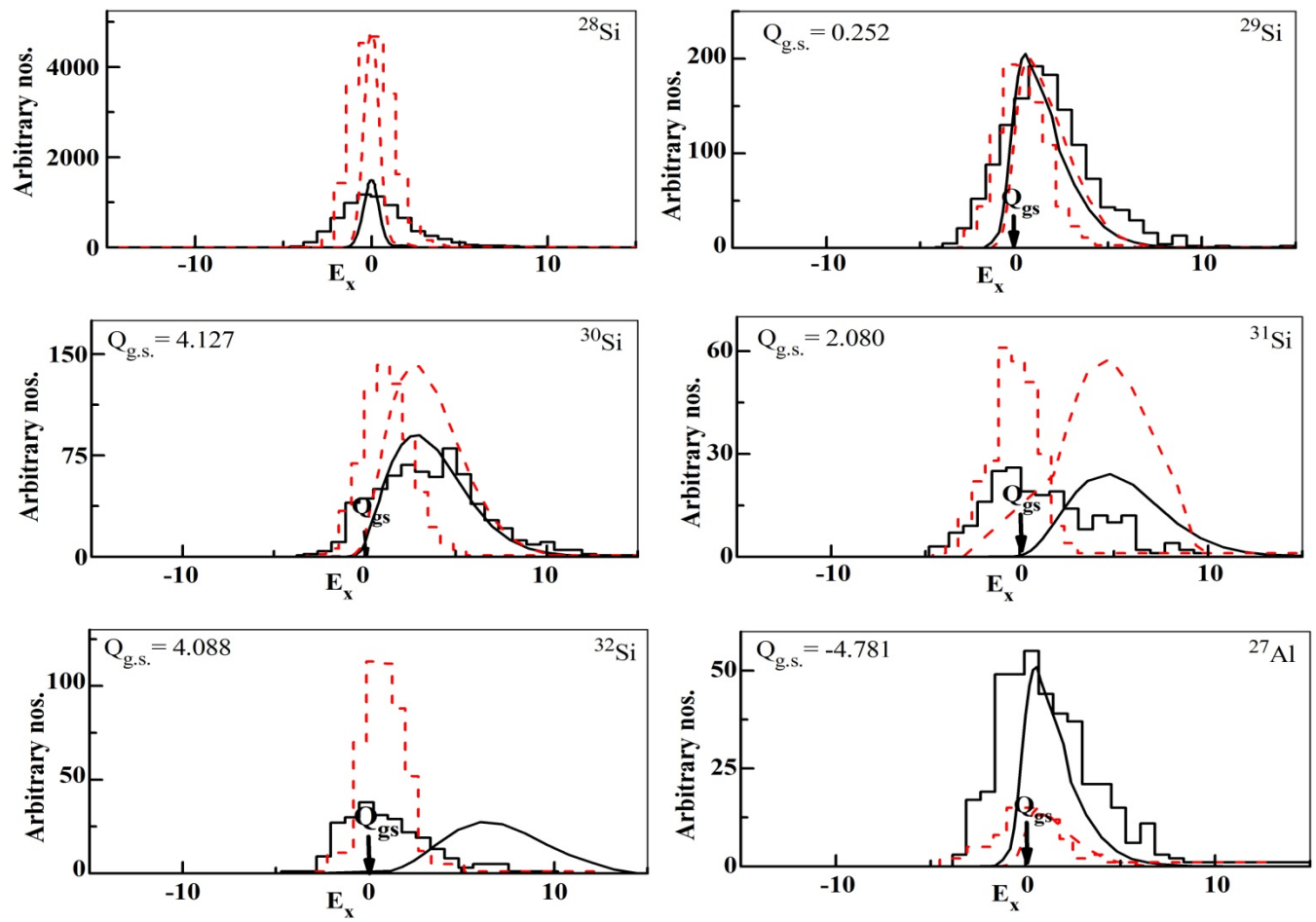


FIG. 6.

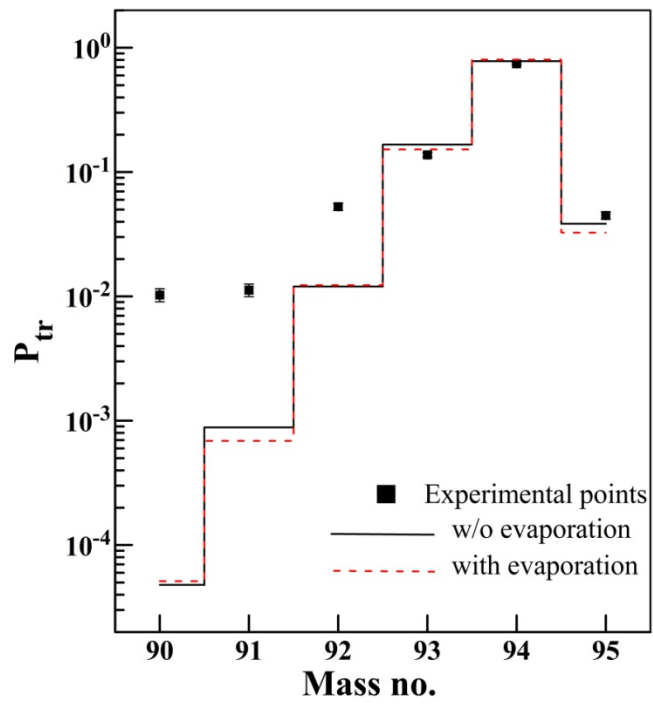


FIG. 7.